Retinal Intrinsic Optical Signals in a Cat Model of Primary Congenital Glaucoma

Jesse B. Schallek,[1] *Gillian J. McLellan,*[2] *Suresh Viswanathan,*[3] *and Daniel Y. Ts'o*[4]

Purpose. To examine the impact of reduced inner retinal function and breed on intrinsic optical signals in cats.

Methods. Retinal intrinsic optical signals were recorded from anesthetized cats with a modified fundus camera. Near infrared light (NIR, 700–900 nm) was used to illuminate the retina while a charge-coupled device (CCD) camera captured the NIR reflectance of the retina. Visible stimuli (540 nm) evoked patterned changes in NIR retinal reflectance. NIR intrinsic signals were compared across three subject groups: two Siamese cats with primary congenital glaucoma (PCG), a control Siamese cat without glaucoma, and a control group of seven normally pigmented cats. Intraocular pressure (IOP), pattern electroretinogram, and optical coherence tomography measurements were evaluated to confirm the inner retinal deficit in PCG cats.

Results. Stimulus-evoked, NIR retinal reflectance signals were observed in PCG cats despite severe degeneration of the nerve fiber layer and inner retinal function. The time course, spectral dependence, and spatial profile of signals imaged in PCG cats were similar to signals measured from normal and Siamese control cats.

Conclusions. Despite increased IOP, reduced nerve fiber layer thickness and ganglion cell function, intrinsic optical signals persist in cats affected with PCG. The mechanisms giving rise to intrinsic signals remain despite inner retinal damage. Signal strength was reduced in all Siamese cats compared to controls, suggesting that reduced intrinsic signals in PCG cats represent a difference between breeds rather than loss of ganglion cells. These results corroborated previous findings that retinal ganglion cells are not the dominant source of intrinsic optical signals of the retina. (*Invest Ophthalmol Vis Sci.* 2012;53:1971–1981) DOI:10.1167/iovs.11.8299

An emerging field in functional retinal imaging has been the investigation of intrinsic optical reflectance signals in the retina. Several groups have reported that presenting patterned visual stimuli to the eye evokes changes in near infrared (NIR) reflectance of the retina.[1–10] The patterned NIR reflectance shows tight colocalization with the stimulated region of retina. Recent reports have focused on identifying the biophysical origins leading to these functional activations.

Investigations using a variety of techniques, including in vitro analysis in the flatmount preparation,[3,4,9] in vivo depth-resolved analysis in the human retina,[10] comparison to laser Doppler flowmetry recordings,[11] and pharmacologic blockade to selectively suppress specific retinal laminae,[6] have revealed several contributing components to the optical reflectance signals. However, debate has arisen regarding the contributions of ganglion cells to these intrinsic signals. Previous work from our group has shown that signals persist after intravitreal injections of agents that block inner retinal function, including tetrodotoxin (TTX), metabotropic glutamate receptor agonist, 2-amino-4-phosphonobutyric acid (APB), and the ionotropic glutamate receptor antagonist, *cis*-2,3-piperidinedicarboxylic acid (PDA). Given that the functional signals remain after pharmacologic suppression of inner retinal activity, it was concluded that signals arise primarily from the outer retinal layers.[6] Data from another study, however, has shown that intravitreal injections of TTX produces a measurable reduction in intrinsic signal response.[11] This result from Hanazono et al.[11] suggests that inner retinal function is a major contributor to these signals. To further tease apart the discrepancies in these conflicting results, this study examined intrinsic optical signals in a naturally occurring cat model of glaucoma. In this study, two Siamese cats with a form of primary congenital glaucoma (PCG) were imaged.

These animals show chronic elevation in intraocular pressure (IOP) and consequent loss of inner retinal function, hallmarks that are characteristic of many forms of human glaucoma. Here, spatially-evoked intrinsic signal properties in these cats were compared to the response measured in a control group of healthy, normally pigmented cats and a third Siamese cat with normal IOP. In this report, data were compared regarding the spectral, spatial, and temporal components of the retinal intrinsic signals in these cat groups. The persistence of these intrinsic signals in cats with reduced inner retinal function supports our previous finding that a dominant signal origin lies within outer retinal layers.

Methods

Animals

Ten adult cats between 1.3 and 4.8 years of age were examined. Seven were from a healthy cohort of domestic short-haired cats (*Felis catus*) of normal coat coloration, including tabby and calico (all female; average age: 1.95 years, range: 1.3–3.4 years). These cats served as the control population and collectively will be referred to as "normals." Two seal-point Siamese cats (one male, G1, and one female, G2; average age on date of experiment, 2.0 and 3.5 years, respectively) were from a colony characterized as having naturally occurring, inherited,

From the [1]Departments of Neuroscience and Physiology and [4]Neurosurgery, SUNY Upstate Medical University, Syracuse, New York; [2]the Department of Ophthalmology and Visual Sciences, University of Wisconsin-Madison, Madison, Wisconsin; and [3]Indiana University School of Optometry, Bloomington, Indiana.

Supported by the National Institute of Biomedical Imaging and Bioengineering Grant EB002843 and EY12915 (DYT); the Glaucoma Research Foundation (DYT); and the National Institutes of Health Grant K08 EY018609 (GJM).

Submitted for publication July 26, 2011; revised December 9, 2011; accepted December 28, 2011.

Disclosure: **J.B. Schalleck**, None; **G.J. McLellan**, None; **D.Y. Ts'o**, P

Corresponding author: Jesse B. Schallek, Center for Visual Sciences, University of Rochester, 601 Elmwood Avenue, Box 659, Rochester, NY 14620; jschallek@cvs.rochester.edu.

congenital glaucoma. For brevity, these animals will be referred to as the "glaucoma" population.

These animals present with many of the hallmarks of human congenital glaucoma, an eye disease that typically shows inner retinal damage to retinal ganglion cells and their axons in the retinal nerve fiber layer (RNFL) and optic nerve. Elevation in IOP in these cats results from arrested development of the aqueous outflow pathways early in life. This IOP elevation ultimately leads to moderate buphthalmos and reduced inner retinal function (McLellan GJ, et al. *IOVS* 2006;47:ARVO E-Abstract 175). Though many factors contribute to inner retinal dysfunction, there is agreement that chronically increased IOP is a leading risk factor for the development of glaucoma.

A third genetically unaffected seal-point Siamese cat (S1) was also studied to examine the effects of breed on intrinsic signal properties, independent of increased IOP. The average experimental age for this cat was 3.3 years. All animals were examined with the same experimental apparatus and same technique to restrict confounds of method variability. Both left and right eyes of all animals were examined. All procedures adhered to the ARVO Statement for the Use of Animals in Ophthalmic and Vision Research. Animals were cared for in accordance with the Animal Welfare Act and the "Guide for the Care and Use of Laboratory Animals."

IOP Measurements

Intraocular pressures of awake cats were measured approximately once a week with an applanation tonometer (Tono-Pen XL; Medtronic, Jacksonville, FL). Measurements were obtained at a consistent time of day (2:00 PM–4:00 PM) to reduce variability due to circadian fluctuation in IOP.[12] Cats were acclimated to the procedure and were held gently during IOP measurements to prevent false readings arising from resistance to restraint. Topical anesthetic (proparacaine HCl 0.5%; Bausch & Lomb, Tampa, FL) was applied to the eye and six or more individual readings were obtained from each eye and averaged to represent data from a given day.

Pattern Electroretinogram (PERG) and Optical Coherence Tomography (OCT) Measurements

We used PERG and OCT measurements to provide noninvasive corroboration of ganglion cell deficits in the PCG cats. For both PERG as well as OCT measurements, animals were anesthetized with a mixture of ketamine HCl (20 mg/kg intramuscularly [IM]) and xylazine (3 mg/kg IM) and thereafter maintained with ketamine alone (5 mg/kg IM) as needed. Body temperature was maintained with a water-circulated heating pad and monitored around 37°C. Accommodation of the lens was blocked with tropicamide HCl (1%), and pupillary dilation and retraction of the nictitating membranes were achieved with phenylephrine HCl (2.5%).

For PERG measurements, as previously described by one of the authors,[13,14] the eyes were treated with proparacaine HCl (0.5%), and a fiber electrode (DTL Plus; Diagnosys, LLC, Lowell, MA) moistened with 1% carboxymethylcellulose sodium was centered across the cornea of each eye and covered with a gas-permeable contact lens. The eyes were refracted with a retinoscope, and final focus of the eye on a video display monitor located 50 cm away was achieved with spectacle lenses. A hand-held transilluminator was used to back-project the fundus, check refraction, center the area centralis on the video display monitor, and check eye position during recording. Each eye was tested separately, with the fellow eye covered with a light-proof cloth. The covered eye served as a reference, and a needle electrode inserted under the skin of the neck served as the ground electrode.

Pattern visual stimuli (4700°K color temperature) were displayed on an RGB monitor (model HL7955SKF; Sony, Tokyo, Japan) running at a frame rate of 100 Hz. Stimuli were luminance modulations of either a uniform field or contrast reversal of grating patterns. Square-wave luminance modulations were used in both the spatial and temporal domains. Stimuli of spatial frequencies ranging from 0.063 to 2 cyc/deg were presented at 1 Hz (two contrast reversals per second) temporal frequency, where maximum amplitudes are generated. At the viewing distance of 50 cm, the test field subtended a visual angle of 42° horizontally and 37° vertically. Photopic luminance (in candelas per square meter) was calibrated with a spot photometer (LS-100; Konica Minolta, Ramsey, NJ). The minimum and maximum luminances were 2 and 96 cd/m^2, respectively, resulting in a stimulus contrast of 95%. Signals were amplified, direct-current filtered (300 Hz), and digitized (1 kHz) with a resolution of 0.1 μV. Responses were averaged over 50 stimulus presentations. The largest Fourier component close to 60 Hz was removed digitally to simulate a notch filter, with no phase distortion having a bandwidth of <0.02 Hz. Repeated three-point weighted smoothing (0.25, 0.5, and 0.25) was sometimes used to eliminate noise at frequencies >250 Hz.

In healthy cats, the N95 component (a negative voltage typically observed with a latency approximating 95 ms) in transient PERGs, as recorded in our study, represents inner retinal, and specifically, ganglion cell functional activity.[13,14] N95 amplitudes from glaucoma cat 1 (G1) were compared to normative data from healthy cats (N = 18).

OCT scans of the peripapillary region of a normal cat and the glaucomatous animal were obtained with the Stratus OCT 3000 (software 4.01; Carl Zeiss Meditec, Inc., Dublin CA). The peripapillary Fast 3.4 RNFL algorithm was used. The Fast RNFL scan consists of three peripapillary scans (256 A-scans each) with a nominal diameter of 3.4 mm. RNFLT was automatically determined by the OCT software. The average RNFLT of normal cats was 40 μm.

Imaging Preparation

Animal preparation was as described previously.[5,6] In summary, animals were anesthetized before being placed in a stereotaxic frame. An intravenous infusion of sodium thiopental (1–2 mg/kg/h) was delivered continuously to maintain consistent anesthesia. Cats were endotracheally intubated, then paralyzed with intravenous vecuronium bromide (0.1 mg/kg/h) to minimize ocular movements. Cats were artificially ventilated with room air to compensate for diaphragm paralysis. Vital signs including expired CO_2, body temperature, electroencephalogram, and electrocardiogram were monitored closely to ensure animal vitality during the procedure.

Phenylephrine HCl (10%; Akorn, Lake Forest, IL) and atropine sulfate (1%; Bausch & Lomb) were applied topically to the cornea to dilate the pupil and prevent accommodation. 3+4.0-diopter hard contact lenses were placed on the corneas to prevent drying.

Imaging

The retinal image was captured through a modified fundus camera. A more detailed description has been published previously[5] (also, Ts'o DY, et al. *IOVS* 2009;50:ARVO E-Abstract 4322). Briefly, an internal illumination source was filtered by narrow bandpass filters to produce diffuse NIR illumination of the fundus that was continuously on for the duration of the experiment. Wavelengths tested were 700, 750, 780, 850, and 900 nm (each 10-nm bandpass at full width, half height). In addition to low-power corrective lenses fitted to the cat, the total corrective power of the system was optimized for best focus of the ocular fundus in the NIR bands. Patterned visual stimuli (bars or spots of 540 ± 30 nm light) were presented in a randomized block trial format. Luminance of the stimulus was 7cd/m^2 and produced a Michelson contrast of >95% against background levels. The NIR reflectance of the fundus was recorded with a CCD camera (Photometrics Ltd., Tucson, AZ). The field of view captured by the camera spanned 35°, centered 0° to 30° from the area centralis. Reflectance images were acquired at a rate of 2 Hz. A single acquisition consisted of a continuous recording of 2 seconds of prestimulus reflectance, 3 seconds of stimulation with 540-nm patterned light, and 5 seconds of poststimulus recovery. Twelve seconds or more were allowed between subsequent stimulus presentations to allow for adequate signal

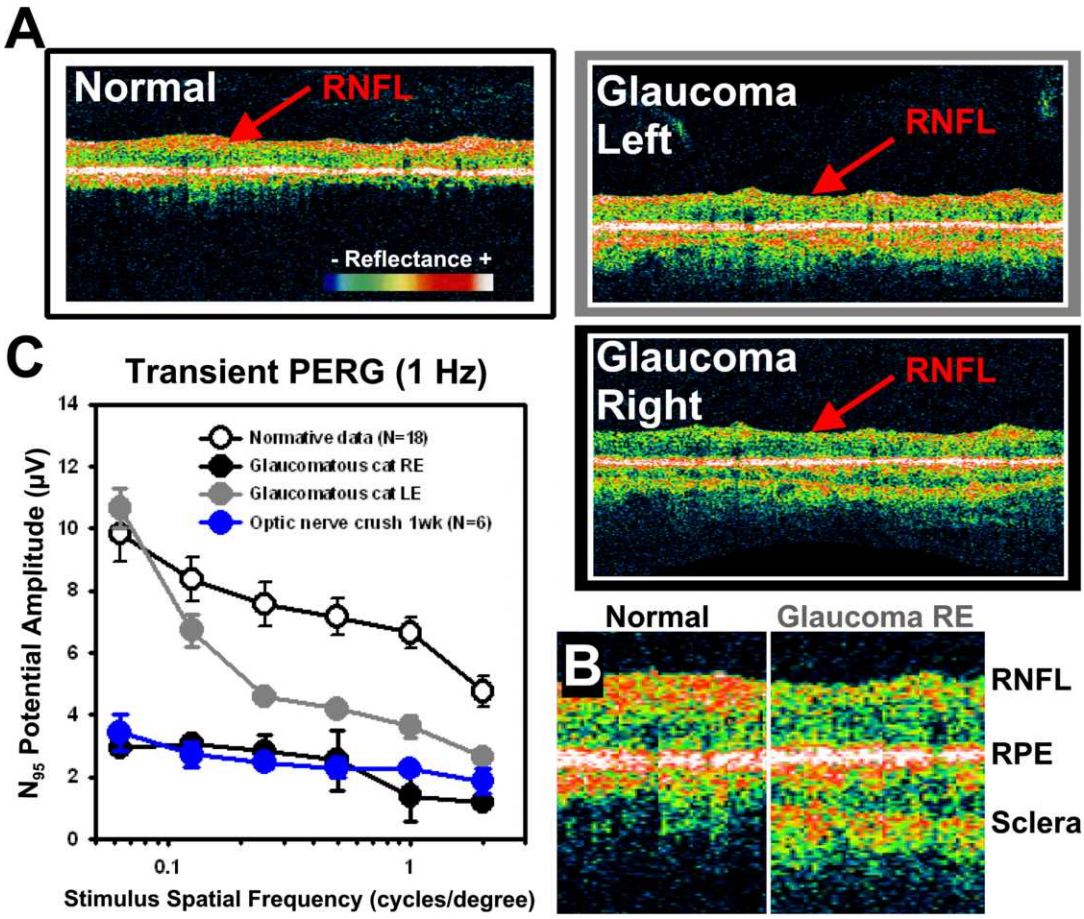

Figure 1. PERG and OCT data. (**A**) OCT peripapillary B-scans (Stratus; Carl Zeiss Meditec, Inc., Dublin, CA) show optical reflectance of specific retinal layers in vivo. Scans of normal cat retinas show strong reflectance arising from the RNFL (red arrow). A representative scan from glaucoma subject 1 (G1) is shown at right. Pronounced thinning of the RNFL was observed in both the left eye (LE, top) and especially the right eyes (RE, bottom). Retinal scans are magnified and aligned to RPE density in (**B**). RNFL showed reduced density despite relatively normal retinal thickness and reflectance of middle and inner layers (regions between RNFL and RPE). (**C**) PERG amplitude. The N95 component of the PERG response was plotted as a function of spatial frequency for four data sets. Normal feline PERG amplitudes (open black symbols) are significantly greater than either of the recordings of LE or RE recordings of subject G1 (closed gray and black symbols, respectively). The average N95 PERG responses of a normal cat subject to an optic nerve crush experiment are shown in blue for comparison. The error bars represent the standard error from the mean.

recovery. Four acquisitions from the same stimulus condition were averaged together to produce one data file stored for offline analysis. Imaging protocols and recording conditions were kept consistent between recording sessions and for all cats. Cats were imaged no more than once per week to allow sufficient recovery between imaging sessions

Intrinsic Optical Signal Analysis

The reflectance changes are small when compared to background illumination. To reveal the optical changes, a baseline reflectance frame (R) was subtracted from all subsequent frames in a given imaging acquisition (change in reflectance reported as dR). The difference frames (dR) were divided by the baseline reflectance frame to provide the fractional change in reflectance (dR/R). Images presented in this report showed a fixed grayscale range, where midlevel grays represent dR/R = 0, that is, no reflectance change. Brighter values represent relative increase in reflectance and darker values represent a relative decrease in reflectance. Time course and magnitude data report the averaged responses from user-defined regions of interest (ROIs). Typical ROIs were 11×11-pixel windows (1.5° to 1.9° visual angle) centered over strong activation regions. The same analysis region was examined for all illumination wavelengths examined. A more detailed description of analysis methods has been reported previously.[5,6]

Results

PERG and OCT

The left and right eye of glaucoma subject G1 showed reduced density and thickness of the RNFL related to loss of ganglion cell axons (Figure 1A). Decreased reflectance from the RNFL was most pronounced in the right eye of this cat. A magnification of OCT data from the right eye of a normal and a glaucoma cat is shown in Figure 1B. The thickness and density of the neural retina was comparable between normal and glaucoma cats, with the exception of decreased reflection from the RNFL in glaucoma cats. The average RNFL thickness of normal cats was 40 μm; the average RNFL thickness of the right eye of G1 was 20 μm, whereas the left eye was 8 μm. This is also consistent with reports of inner retinal damage in human glaucoma.[15]

A representative normal cat N95 potential to several spatial frequencies is shown with open symbols in Figure 1C. The N95 component of the left and right eye of subject G1 showed markedly reduced N95 potentials, consistent with markedly reduced ganglion cell function of optic nerve crush experiments.[16,17] Moreover, the severity of functional loss in this subject mirrored the anatomic deficits observed in OCT scans

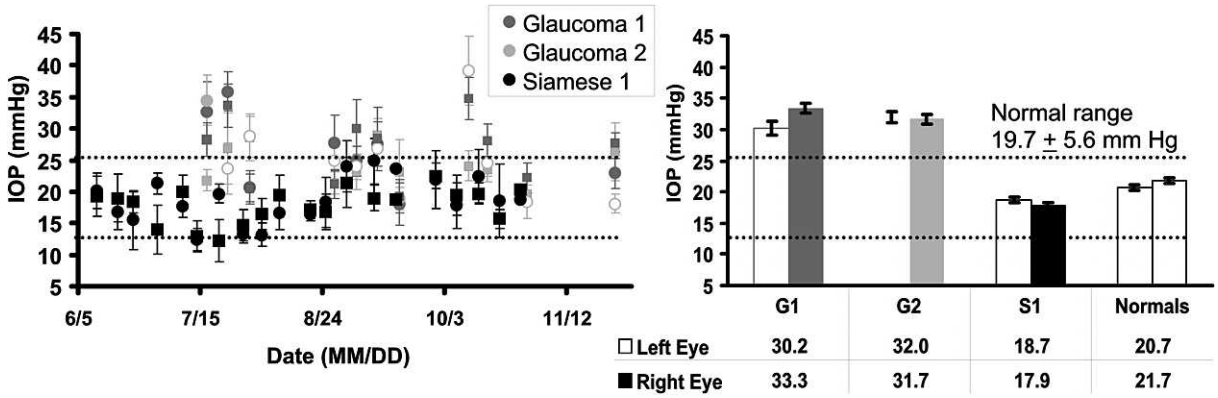

Figure 2. Intraocular pressure data over the course of the study. (**A**) IOPs were measured for three cats over the course of 4 to 5 months. Data from glaucoma cats are shown in shades of gray, while data from a Siamese control are shown in black. Each data point represents the average of at least six readings, error bars show ±1 SD. Left eye data are represented by a circle, and right eye, designated by squares. The dotted lines represent the limits of the reference range for IOP in normal cats. Most of the data from cats showing a glaucomatous phenotype are higher than the normal range. Data from the control Siamese are within the normal reference range. (**B**) Average IOP measurements. Data from (**A**) were averaged over all measurements during the 4 to 5 months over which the cats were imaged. Left eye data are represented by striped bars, right eye data are represented by solid bars. Glaucomatous cats show consistently elevated IOP, whereas the control Siamese and other normal cats had IOPs within the normal reference range. Similarly, the collective average from three representative normal cats is shown in white at right. Error bars in B show ±1 SEM for each subject G1, G2, and S1 (where G represents glaucoma and S represents Siamese control). The normal cat data at right represents a pooled average of all recordings taken in three normally pigmented cats (normals); thus, inter- and intrasubject variance is represented within the error bars. The table under Figure 1B shows average IOP (mm Hg) for each cat group.

(Figure 1A). The glaucoma right eye potential (black data) was more severe than the left eye (gray data) deficits, which correlate well to the anatomic loss of the RNFL in OCT scans from the same animal (Figure 1B, 1C). For comparison purposes, the PERG response from an unrelated experiment, where the optic nerve was crushed, is shown in blue. Several weeks after the mechanical crush of the optic nerve with forceps, the ganglion cell population in this animal was devastated owing to retrograde degeneration arising from the crush of its axon projections.

Intraocular Pressure

Both cats with PCG had consistently increased IOP compared to the control Siamese and normal cats. Figure 2 shows IOP measurements from three cats over the course of 4 to 5 months. Average IOP was elevated, ranging from 30 to 33 mm Hg in both eyes over the course of this investigation, which is considerably higher than the reported normal range of IOP in healthy cats (19.7 ± 5.6 mm Hg [average ±1 SD]) reported by Miller et al.[18] in 1991or Rusanen et al.[19] in 2010 (mean IOP, 18.4 mm Hg). Data from cats with PCG (dark gray, and light gray data) generally showed IOP readings above the normal reference range for healthy cats[18] (19.7 ± 5.6 mm Hg, shown as dashed horizontal lines in Figure 2A). Conversely, IOP from a Siamese control cat obtained over the 5-month period showed average IOP of 17.9 and 18.7 mm Hg (left and right eye, respectively) and generally fell within the normal range for feline IOP. The glaucomatous cats tested showed bilateral elevations in IOP that were relatively symmetrical (Figure 2A). Figure 2B shows the average of all recordings in each cat group. On average, glaucoma cats (gray bars) showed increased IOP of 30.2 to 33.3 mm Hg, exceeding the normal range. In contrast, the Siamese control from the same breed (cat S1, black bars) had IOPs within the normal range. For reference, average IOPs pooled from three normal cats were also graphed (white bars). As expected, our normal control population had readings within the healthy range of feline IOPs.[18]

Spatial Properties of Intrinsic Signals

When presented with patterned visual stimuli, spatially specific activations in all cats imaged were observed. Representative examples of the signal response to three stimulus conditions are presented in Figure 3. All images were plotted on the same grayscale range to show relative signal strengths across groups.

As observed in previous reports, a negative signal corresponding to a stimulus-evoked decrease in reflectance relative to a baseline state is colocalized with the stimulated region of retina. A positive signal, corresponding to an increase in reflectance, is often observed adjacently (Figure 3A, bottom row).

Signals in Siamese cats with chronically elevated IOP and normal IOP appeared qualitatively similar to signals typical of normals (left). The signals recorded in the Siamese cats had the same spatial attributes as the normals. A negative signal underlies the stimulated region of retina, while a positive signal emerges nasal to the stimulated region. Upon quantitative inspection, the signals from both the glaucomatous and control Siamese cats, irrespective of IOP, had decreased signal magnitude when compared to the normals. This can be seen by the stronger signal deflection from zero within the locked grayscale range of ±0.007 dR/R. The signal was stronger in the normal cats than in either the glaucomatous or normotensive Siamese cats.

The differences in spatial signal amplitude are further demonstrated in Figure 3B, where a line profile of the signal is shown. A cross-sectional profile of the signal was plotted from the boxed region in the bottom figures in Figure 3A. Normal cats showed a strong negative activation with a positive deflection on the nasal side. The same trend in signal profile was seen in Siamese cats with either normal or high IOP.

Signal Line Spread

A detailed analysis of the cross-sectional profile was performed to characterize line spread properties in the three cat groups. Representative cross-sectional data in Figure 3B were normalized for comparison in Figure 4. Signals from normals, PCG,

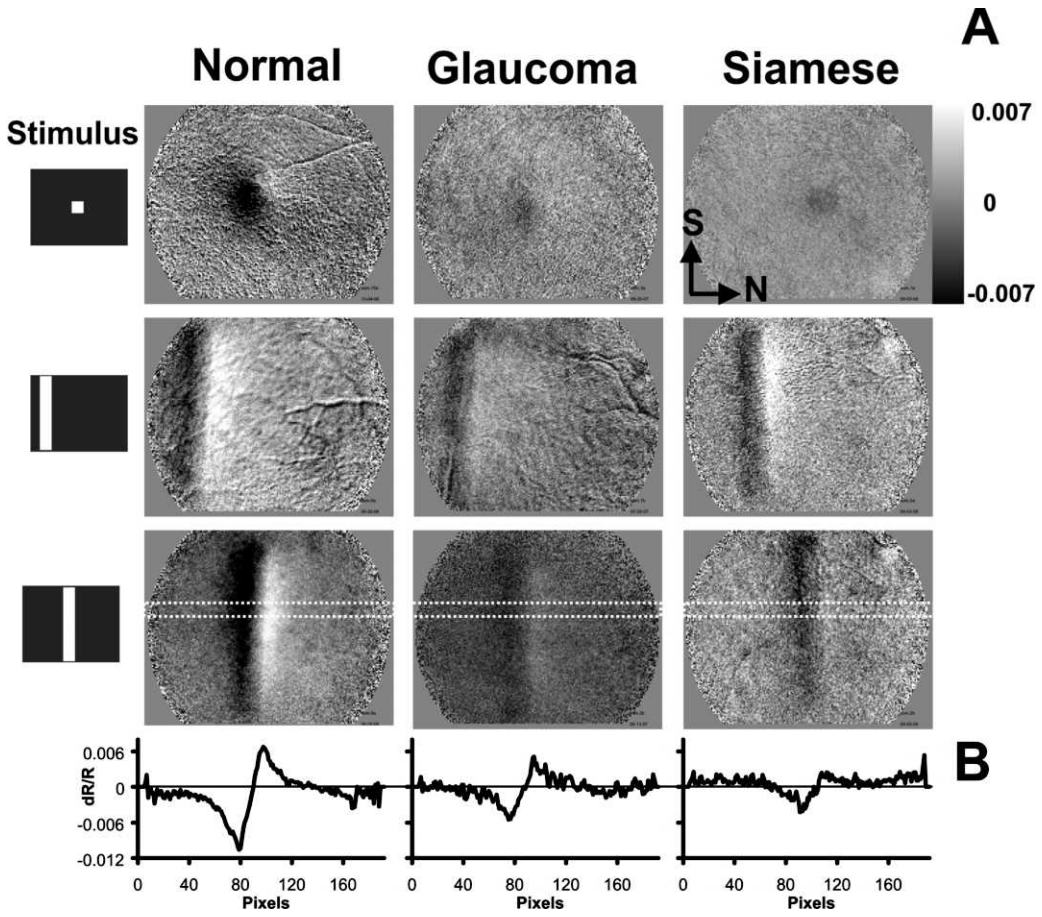

Figure 3. Intrinsic optical signal spatial response. (**A**) Representative images from normal (left), glaucomatous (center), and Siamese control cats (right). Data show the retinal NIR response to three stimulus conditions, a spot stimulus (top), and two horizontally displaced vertical bars (middle and bottom). Data are from t = 5.0 to 6.0 seconds (just after stimulus presentation epoch, when signals are strongest). In all three cats, intrinsic signals are present that show a characteristic patterned response to the stimulus. All images are plotted on the same grayscale range (±0.007 dR/R). Normal cats show stronger activations in both the negative and positive signals, represented by more pixels reaching a saturated state within the grayscale limits. (**B**) A cross-sectional profile of intrinsic signal. An 11×192–pixel region (dotted trace in bottom of **A**) was averaged in the short dimension from the vertical bar condition in the lower panels of (**A**). Intensity data are now represented by the ordinate dimension (dR/R), and abscissas show distance in pixels in the nasal–temporal axis. Negative and positive signals are observed in each cat. Positive signals generally show a nasal bias to the negative signals. Slight shifts in signal position are due to positional variations of the stimulus within the field of view. Nasal (N) and superior (S) directions are shown in top right image for orientation.

and normal Siamese cats were normalized to either the positive peak (top) or negative peak (bottom). The data were then aligned in the abscissa dimension to the prominent negative peak to correct for slight positional variation of the stimulus relative to the field of view. The normalized data showed strong overlap of the cross-sectional profile from all populations of cats. To quantitatively measure the signal spread, an analysis of the signal of the full width was performed, at half the height of the amplitude (FWHH). This analysis shows the lateral spread in the signal in the nasal–temporal axis. Positive signals showed a width of 2.19° to 3.09° of visual angle. Negative signals showed widths of 2.55° to 3.28°. Visual angle measures were converted into dimensional space by using a conversion factor from Vakuur et al.[20] With this criterion, positive signals were 477 to 676 μm FWHH and negative signals, 557 to 716 μm FWHH across groups. The spatial width of the signals in each group showed strong similarity, especially considering that the optimal point-spread resolution of the technique has been approximated at 80 μm, calculated in a unidirectional profile (Ts'o et al. *IOVS* 2009;50:ARVO E-Abstract 4322).

When negative signal peaks were aligned along the abscissa, high precision of negative to positive peak alignment across cat groups was found. In particular, the transitional zone between negative and positive peaks was notably similar (between vertical dashed lines in Figure 4). The peak-to-peak distance was 836 μm (3.83°) in each cat group imaged, indicating a similar and intact spatial mechanism for both the positive and negative signal in all cats imaged.

Time Course Analysis

An analysis of the time course of signal from normal Siamese and glaucoma cats showed that signals retained the same general shape as the normals. Figure 5 shows averaged signals for each of the 700- to 900-nm wavelengths, examined from the three cat populations. As reported previously in the normal cat, signals are strongest at the shorter end of the NIR spectrum, and smallest at the longest wavelengths, while retaining a similar monophasic growth and decay function.[5] Averaged responses of each of the NIR wavelength filters used between 700 to 900 nm were plotted for the normal cat in Figure 5 (right), and were similar for the normal Siamese and

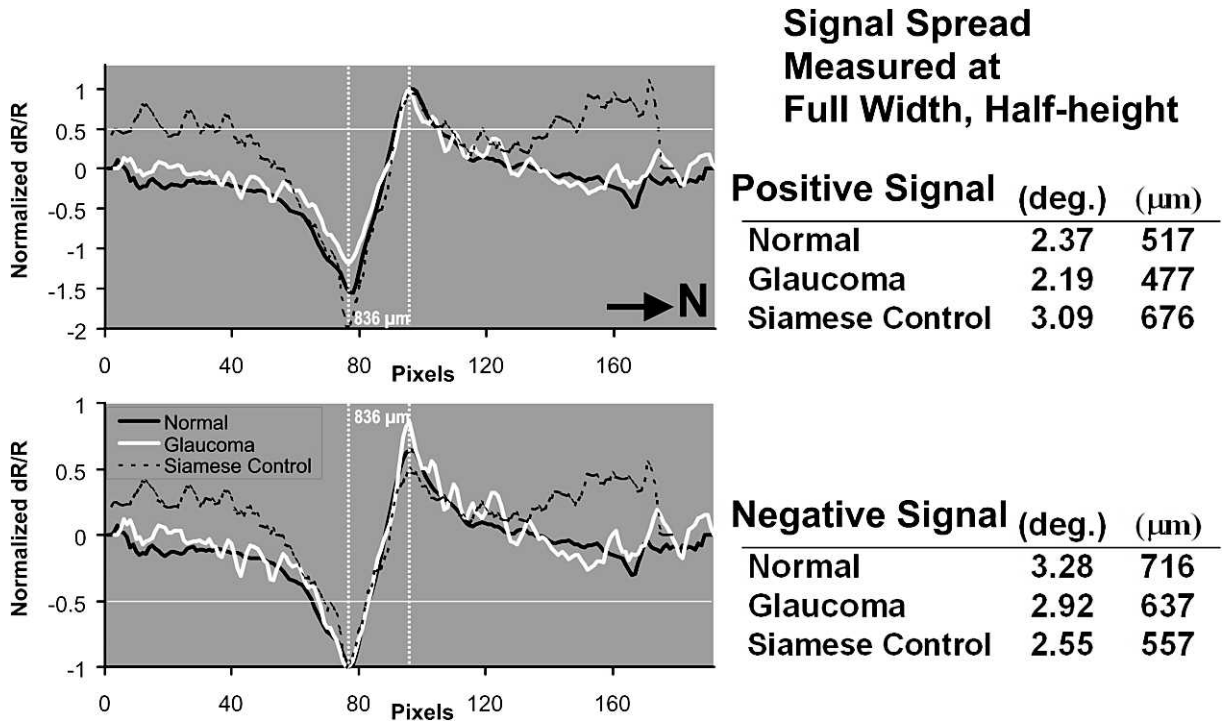

Figure 4. Point spread analysis of signal in three cat populations. Representative data from Figure 3 are normalized to either positive peak (top) or negative peak (bottom) to reveal point-spread properties of the response. Slight positional variations of the stimulus relative to the imaged field of view are corrected by aligning the peaks along the abscissa. Normal data (black), glaucoma data (white), and Siamese control (dotted) show strong overlap of the signal profile. When normalized to either the positive or negative peak, full width at half height (horizontal line) shows good agreement of signal spread. Tables at right report signal width at half height in degrees and micrometers of retinal distance. Both positive and negative peaks show the same displacement when abscissas are aligned to the opposite polarity (vertical lines show alignment of peaks). Black arrow signifies nasal direction (N).

PCG cats. The general shape of the growth and decay functions, although reduced in amplitude, was preserved in normal Siamese and PCG cats. The time course of all data remained consistent across cat populations, where two seconds of prestimulus is associated with minimal change in reflectance, three seconds of stimulus produces a monophasic growth function, and signals begin to recover approximately 0.5 to 1.5 seconds after stimulus offset. In Figure 5, the observed response was averaged for each cat, producing a single time course for that wavelength. Since there was only one cat in the Siamese control group, the error bars represent a measure of the observational variance with repeated stimulus presentations on five experimental dates. In the case of the glaucoma cats and normals, the mean response for each cat was averaged, producing a single time course for the corresponding wavelength. These data were then averaged in each cat group (n = 7, normals; n = 2, glaucoma) for each wavelength and plotted in Figure 5. Here, the error bars represent variance across individuals. In either case, error bars represent ±1 SEM. Though reduced in amplitude, Figure 5 shows that these cat groups generally show similar onset, growth, and decay functions.

Data from Figure 5 are examined in detail in Figure 6 for wavelengths 700, 750, and 800 nm to disambiguate the traces in Figure 5 and reveal subtle differences. Figure 6 shows population-averaged data from normals, glaucoma cats, and Siamese control. This magnified inspection at these wavelengths shows that the shape of the time course in glaucoma

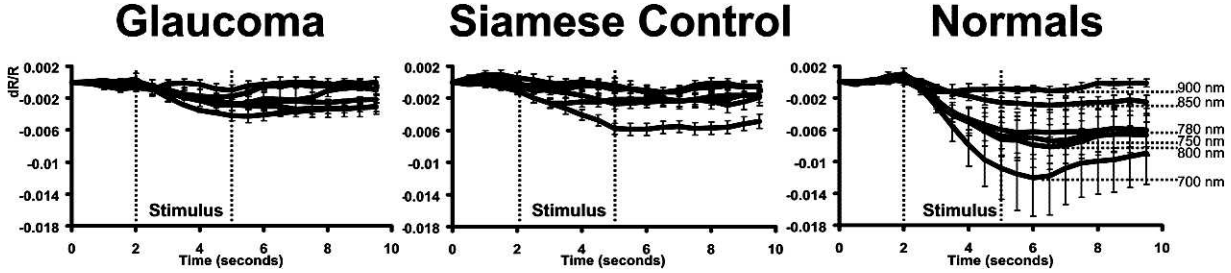

Figure 5. Average signal time course for wavelengths 700 to 900 nm. The averaged data from two glaucoma cats, a Siamese control, and seven normals are plotted. The wavelength dependence is represented for the normal data at right. The general shape of the intrinsic signal development remains the same for all cats tested despite reduced magnitude observed in Siamese and glaucoma cats. In this figure, signals show a similar onset, monophasic growth function and poststimulus decay period linked to the phase of the stimulus epoch (vertical lines). The specific wavelength dependence for glaucoma and Siamese controls is disambiguated in following figures. Error bars represent ±1 SEM of all averaged data from each cat group.

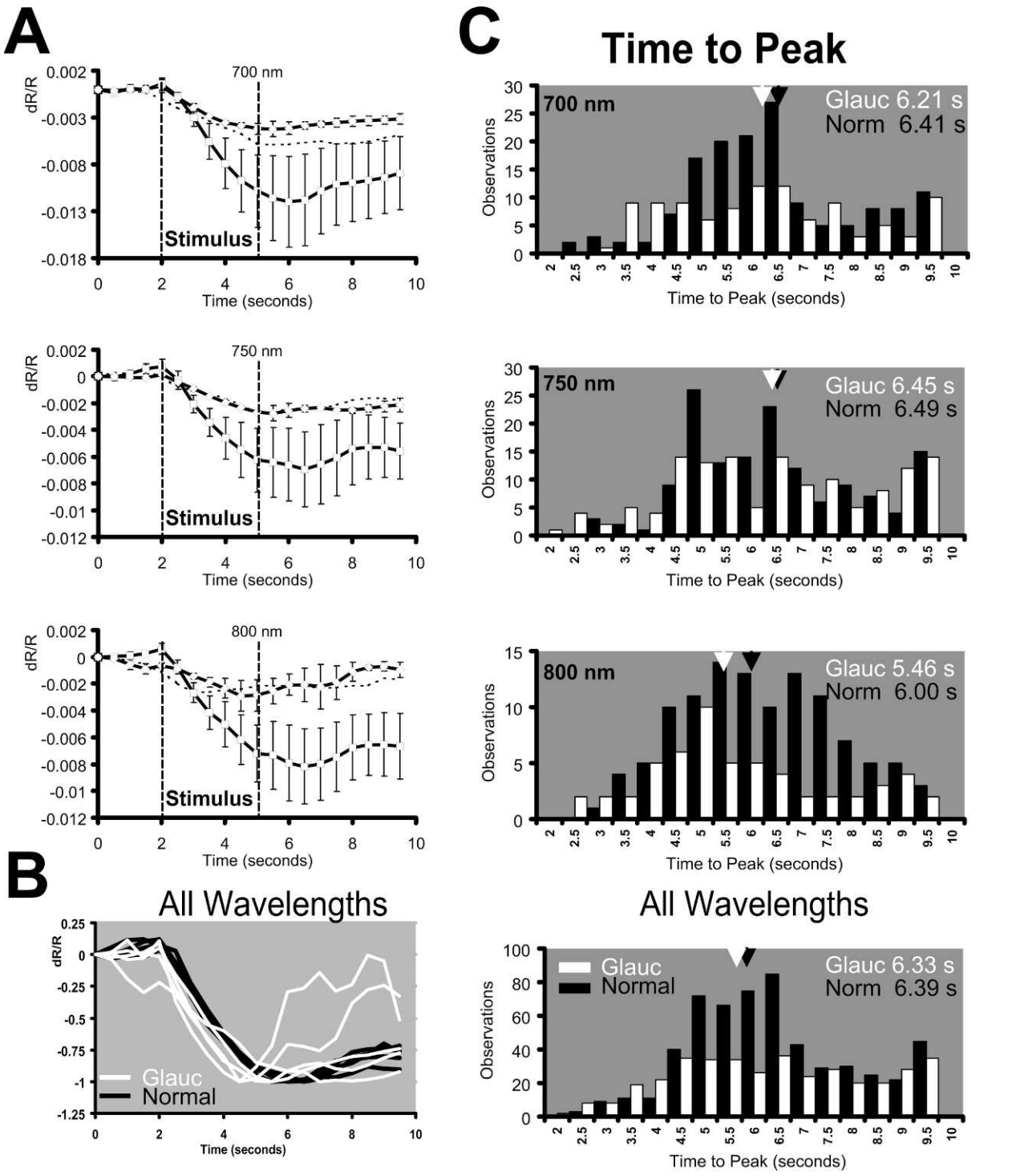

Figure 6. Time course analysis. (**A**) Average intrinsic signal time course for three representative wavelengths: 700, 750, and 800 nm. Data from normals (squares), glaucoma (diamonds), and the Siamese control (dotted line) are plotted. Each cat group showed similar slow onset first detectable from 0.5 to 1.0 second after stimulus onset. All signals grow monophasically for the duration of the stimulus epoch and peak 0.5 to 1.0 second after the stimulation is extinguished. The same general trend is observed across all cats, and all imaging wavelengths. Error bars represent ±1 SEM. (**B**) All data from wavelengths between 850 to 700 nm were pooled across the glaucoma (white) and normal cat groups (black). The response to each wavelength was then normalized and plotted on the same coordinates to show the similarities in signal time course without factoring intensity. In this averaging paradigm, a slight time-advance of the glaucoma data appears. (**C**) Time-to-peak analysis for glaucoma and normal cats. The time-to-peak for each acquired signal was performed to produce a single observation. Histograms show the distribution of individual time-to-peak analyses for 700 nm (top), 750 nm (middle), and 800 nm (bottom). Mean time-to-peak is represented by an arrowhead with adjacent text inset for normals (black) and glaucoma (white). A slight time advance of the signal peak was observed in the glaucoma cats, but did not reach statistical significance. Pooled observations across all wavelengths between 850 to 700 nm were analyzed in the bottom panel of (**C**) where the population shows 402 total observations for glaucoma cats and 592 total observations for normal cats.

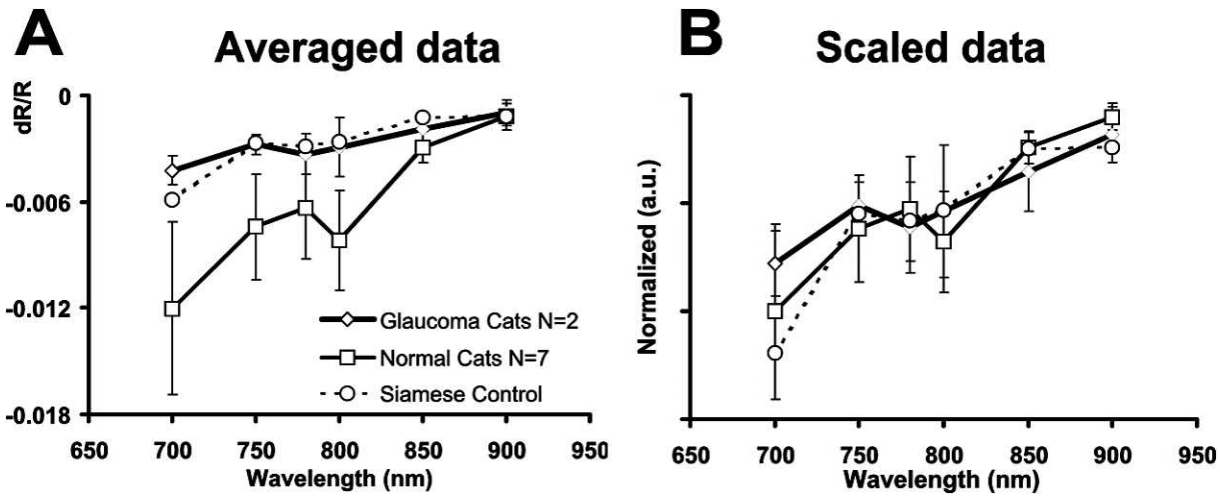

FIGURE 7. Intrinsic signal wavelength dependence across cat groups. (**A**) The average signal for each imaged wavelength was calculated for each cat. The maximum signal deflection of these averages is plotted as a function of wavelength. Normal cats show greatest signals at the shorter end of the spectrum and show decreasing signal strength at progressively longer wavelengths. This trend was also observed for Siamese cats and glaucoma cats despite overall reduced signal strength. Error bars represent ±1 SEM, where N represents the number of subjects in each group. (**B**) Linear transform of wavelength-dependent data. A single conversion factor was applied to the glaucoma and Siamese cat data to compensate for intensity loss. The conversion factor was based on the average percentage reduction in signal strength at imaged wavelengths between 700 to 850 nm. The single scaling factor produced an adequate correction for losses observed in the glaucoma and Siamese cat wavelength-dependent spectra.

cats was largely the same as in normals despite a reduction in signal strength. At each wavelength, signals showed a relatively monophasic growth function and recovery beginning within seconds of the stimulus offset. Importantly, it can be appreciated in Figure 6A that at each wavelength, the time course and magnitude of the Siamese control more closely follows the response to the data from the glaucomatous Siamese cats than the normals at each wavelength examined.

To view differences in time course—independent of magnitude—we normalized the average signal to the maximum deflection Figure 6B. Here the average data from 700, 750, 780, 800, and 850 nm were plotted for normals and glaucoma cats. Data from 900 nm was excluded owing to insufficient signal-to-noise, where the scaling factor exacerbated the noise rather than normalizing the signal. Consistent with previous findings,[5] the time course in normal animals retained the same general shape regardless of NIR wavelength. Data from 700 to 850 nm conform into a single uniform trace for normal cats (Figure 6B). When the same analysis was done on the average glaucoma cat data, the shape of the intrinsic signal time course remained generally the same. A closer inspection of Figure 6B shows a slightly faster time-to-peak for glaucoma data.

To explore this further, a time-to-peak analysis was performed for each individual observation on each cat (Figure 6C). Here a single "observation" was a signal time course in response to a stimulus condition for a given wavelength (average of four acquisitions, i.e., block trial configuration). From these individual observations, the time point when the signal reached maximum deflection was reported as a single observation at the corresponding frame number. Using this calculation of time-to-peak produces a histogram of the population of observations in all cats for a particular wavelength.

The histograms of data from the 700-, 750-, and 800-nm conditions revealed that glaucoma cats (white bars) showed a slightly faster time to peak than the normal data (black bars). The mean time-to-peak was plotted by an arrowhead above each histogram. In particular, data from 800 nm showed a shift in the mean response of more than 0.5 seconds, while temporal shifts at other wavelengths were less prominent (750 nm).

When all observations are combined from 700 to 850 nm (Figure 6C, bottom) the shorter time-to-peak was less prominent. In this figure, the histogram shows the response from 592 observations in normal cats and 402 observations in glaucoma cats. Average time-to-peak for glaucoma cats was 6.33 seconds, whereas for normals it was 6.39 seconds. The small difference in time-to-peak therefore did not meet statistical significance at the $P < 0.05$ level. Therefore, our data did not show a significant variation in signal time course when comparing glaucoma cats to normal data.

Imaging Wavelength Dependence

In order to examine potential spectral differences in the signals in each cat group, the signal dependence on illumination wavelength was tested. Illumination wavelength was changed in a randomized fashion, while all other imaging and stimulus parameters were held constant. The population-averaged intrinsic signal strength was plotted in Figure 7 as a function of wavelength for the three different populations. Intrinsic signals from the normal cats showed decreasing signal strength with increasing wavelength, a result consistent with our previous observations.[5] As noted in previous figures, glaucoma cats showed a reduction in signal strength across all wavelengths. Signals from glaucoma cats were on average 35.2% to 81.6% the magnitude recorded from normal cats. Similarly, the normal Siamese cats were 44.0% to 99.8% of normal signal magnitude. Largest percentage changes were seen at the 700-nm end of the spectrum, while signals at or near 900 nm showed values similar to normal, representing 81.6% and 99.8% of normal values for glaucoma and control Siamese cats, respectively.

A two-sample t-test was performed to test for a significant difference between glaucoma and normal cat data. The difference in population data did not reach statistical significance for any of the tested wavelengths, suggesting that glaucoma cats did not show a significant decrease in signal strength when compared to normals ($P < 0.198$ at 700 nm, $P < 0.187$ at 750 nm, and $P < 0.122$ at 800 nm). Notably, however, access to only two glaucomatous animals was possible at the time of this study. A further study including more animals with

PCG may increase the statistical power to detect a significant difference between the PCG and normal cat data.

Averaged across all wavelengths, signal strength was approximately half as much as in normals in both glaucomatous and normal Siamese cats (51.3 ± 7.8%, mean ± 1 SEM, and 50.8 ± 10% reduction, respectively). Given the apparent multiplicative consistency in reduction, a simple linear multiplier was applied to the glaucoma and Siamese cat data, based on the average percentage reduction between 700 to 850 nm. Excluding the data at 900 nm due to low signal-to-noise ratio, scale factors were 2.21 for the glaucomatous cats, 2.43 for Siamese control, and 1.0 for the normal cats (i.e., no scaling). The normalized spectral data are seen in Figure 7 (right). This simple multiplicative transform uniformly scales Siamese cat signals to nearly equivalent normal cat values. This suggests that the reduced signal strength likely represents a reduction in a single biophysical mechanism. This result is consistent with the unchanged time course observed in Figures 5 and 6.

Discussion

A central finding in this investigation was that retinal intrinsic optical signals persist in a cat model of glaucoma. Considering that stimulus-evoked signals were still present in cats that had notable structural and functional loss of ganglion cells, as measured by anatomic and functional means (OCT and PERG), our findings corroborate previous findings that the dominant intrinsic signals arise from outer retinal function.[6]

OCT images showed primarily a loss in RNFL reflectance signal intensity (Figure 1). RNFL represents the axon projections from ganglion cells; therefore, normal ganglion cell numbers are likely reduced, though the OCT measurements in this study did not provide sufficient resolution to image the ganglion cell layer directly. Nonetheless, glaucoma cats had markedly compromised ganglion cell function, as measured by PERG. Measurements from the left eye of a PCG Siamese cat G1 had devastated PERG function, similar to amplitudes seen from optic crush experiments using the same PERG recording parameters.[17] These data show that both optic nerve crush and glaucoma data have an approximate 3-fold reduction in N95 amplitude, serving as a functional indicator of marked ganglion cell loss. Consistent with these measurements, subsequent histopathologic evaluation was performed more than 1 year after imaging, and retinal sections revealed pronounced loss of retinal ganglion cells and their axons (forthcoming publication). However, it is not possible to confirm whether the observed pathologic process was present at the time of imaging or represented the progression of disease in the intervening year.

Despite these indicators of severely reduced ganglion cell function, intrinsic signals were still present in glaucomatous cats. The dominant mechanisms giving rise to intrinsic signals remain intact regardless of inner retinal function. These findings are supported by several observations.

The mechanisms giving rise to the signals persist within a similar spatial scale. Difference images and line profile analyses each show that signals of both polarities are present in Siamese cats and retain the same spatial distribution compared to normals (as shown in Figures 3 and 4). This implies that the operant mechanism giving rise to the signals is present in Siamese cats regardless of elevated IOP or ganglion cell loss. The persistence of the signal in glaucoma cats, the preserved spatial organization of the positive and negative signal, along with the similarities in the point-spread functions and the identical nature of the peak-to-peak spatial response, indicate that the mechanism of action remains in Siamese cats, albeit with decreased signal strength. The time course of activation also remains the same in PCG and Siamese cats, indicating that the dominant mechanism retains the same temporal growth and recovery functions. Additionally, the signal spectral dependence on imaging wavelength was similar across normals and glaucoma cats, suggesting that the dominant biophysical origin of the signals remains in cats with reduced ganglion cell function.

Collectively, these data suggest that the operant mechanisms producing signals in normal cats persist in both glaucomatous and normal Siamese cats. This conclusion dovetails with a previous report that shows intrinsic signals do not demonstrate spatiotemporal frequency tuning,[6] a known functional property of ganglion cells.[21,22] The lack of spatial or temporal frequency tuning suggests an origin other than ganglion cells.

The presence of a signal in glaucomatous cats that had severely depressed PERG and decreased RNFL density corroborates our pharmacologic blockade study[6] in which no significant change in intrinsic signals were found after intravitreal injections of drugs that suppress inner retinal function. In summary, a collection of evidence is amassed against an inner retinal origin: (1) Signals do not show spatiotemporal frequency tuning,[6] a known property of ganglion cells; (2) TTX, a drug that blocks spiking activity of ganglion cells does not alter signal properties[6]; (3) APB and PDA, which suppress retinal function proximal to the photoreceptors, had no effect on signal characteristics[6]; and (4) as shown in this study, a cat model with reduced ganglion cell function still showed retinal intrinsic signals, with similar characteristics to normals. Taken together, these findings suggest that ganglion cells are not the dominant origin of intrinsic signals in the NIR range.

The above evidence is generally inconsistent with a finding from Hanazono et al[11] that suggests that the dominant signal source arises from ganglion cells. The authors report that intravitreal injections of TTX abolish the NIR signals at the posterior pole and optic disc. Several concerns exist with the paradigm presented in that report: (1) The time point at which the authors examine the effect of TTX is a day after the intravitreal injection and it is debatable that the attenuated response could have been a product of secondary changes to the retinal system. And (2), silencing voltage-gated sodium-dependent spiking of ganglion cells does not, by itself, represent ganglion cell loss. The PCG cat model used in the present study serves as a more accurate model to study the effects of loss similar to that observed in late-stage human glaucoma. There are several considerations, however, to examine when comparing the Siamese cat as a glaucoma model. Though the data in this report did not show a statistical difference between the normal cat, normal Siamese, or glaucoma cat populations, there did, however, appear to be a reduction in signal strength in Siamese cats, regardless of glaucoma status. We posit that the differences in signal strength seen in the glaucoma cats are due to a difference in cat breed rather than a reduction of inner retinal contributions. The evidence for this was seen in the similarities in the spatial, temporal, and spectral data of a Siamese control cat compared to the glaucoma data. Figures 3, 4, 5, and 6 all yielded comparable data showing that Siamese cats were similar to each other in each of the characteristics being studied, independent of IOP and presence of glaucomatous damage. In fact, the difference in signal strength averages was smaller when comparing normal Siamese and glaucoma Siamese cat signals than when comparing signal strength between glaucoma and normal cats. Although more subjects are needed to examine the statistical significance of these population differences, the purpose of this study was primarily to show

that signals persist, and that a plausible reason for reduced signals may arise from a difference in breed. This could be further explored by examining intrinsic optical signals in a glaucomatous cat, free of the potentially confounding Siamese phenotype. Although glaucoma segregates in the out-crossed breeding colony independently of eye and coat color mutations, including Siamese, a non-Siamese cat with PCG of the appropriate age for study was not available at the time this study was conducted.

Several reports have identified some key differences in Siamese cat vision when compared to that of normal cats. These include, but are not limited to, behavioral contrast sensitivity,[23] thalamocortical visual projections,[24] nasotemporal divisions of ganglion cell projections,[25] and X- and Y-cell ratios.[26,27] Importantly, it has been shown that despite several anatomic abnormalities in the Siamese cat retina, the total ganglion cell numbers are generally the same as the normal cat retina.[28] In a histologic study, Stone et al[29] show that the Siamese cat retina shows upwards of 130,000 ganglion cells, comparable to similar counts in normal retinas (112,000 to 147,000 ganglion cells per retina). The subtle differences in ganglion cell densities come from reports within the area centralis, the area of highest visual acuity in the cat. By way of comparison, our imaged field of view was typically several degrees temporal to the area centralis, where this and previous reports show strong signal activations[5,6] (also, Ts'o et al. *IOVS* 2009;50:ARVO E-Abstract 4322). Therefore, the reduced signal observed in our Siamese control cat is not likely a consequence of reduced ganglion cell density/function.

What then are the mechanisms leading to a reduced intrinsic signal in Siamese cats as a breed? The reduced signal could result from pigmentation differences between the cat breeds. Histologic evidence from Thibos et al[30] shows that Siamese cats have reduced RPE thickness (10–20-μm thick in normal cats versus 3–5 μm in Siamese cats). Additionally, that study found reduced pigmentation in the choroid. Reduced pigmentation is consistent with our observation that the Siamese cat fundus required illumination power several orders of magnitude less than that needed to provide comparable reflection in the normal cat retina. This phenomenon was observed despite previous reports that Siamese cats have similar[30] or even reduced tapetal reflectance when compared to normally pigmented cats.[31] Therefore, the increased fundus reflectance in Siamese cats likely results from decreased RPE or choroidal absorbance (whereby less absorbance leads to increased net reflectance). Because functional contrast is mediated by changes in tissue reflection and absorption, decreased pigmentation in Siamese cats could be a leading factor of the decreased intrinsic signal.

Additional investigation will be required to further examine the differences in signals between normally pigmented and Siamese cats. For now, however, this report establishes that intrinsic optical signals are present in cats with advanced glaucoma. This is an important finding that corroborates previous claims that intrinsic signals do not arise from ganglion cell function. It also suggests that the dominant intrinsic signals in the retina are poor markers of primary ganglion cell loss. Therefore, early demonstrations of the utility of this technology may not be best suited for diagnosing and monitoring the hallmarks of glaucomatous damage. Yet, if long-term changes occur, which lead to secondary pathology of outer retina due to inner retinal loss, this technology could provide an interesting longitudinal metric for spatial pathology linked to chronic, untreated glaucoma. Alternatively, it may prove to be a useful tool in monitoring other retinal degenerative diseases that primarily affect the photoreceptors and outer retinal layers, such as retinitis pigmentosa. Considering evidence for a hemodynamic component,[7] intrinsic signal imaging may also be useful in diagnosing diseases affecting the ocular vasculature, such as diabetic retinopathy or age-related macular degeneration. Continued investigations will help reveal useful applications for this promising technology for both clinical patients and basic science research.

Acknowledgments

The authors thank Dori Joiner and Sandy McGillis at SUNY Upstate Medical University for their technical assistance; and N. Matthew Ellinwood, Iowa State University, and Arthur Weber, Michigan State University, for their contributions and expertise regarding the Siamese glaucoma and optic nerve crush cat models, respectively.

References

1. DeLint PJ, Berendschot TTJM, van de Kraats J, van Norren D. Slow optical changes in human photoreceptors induced by light. *Invest Ophthal Vis Sci*. 2000;41:282–289.
2. Abràmoff MD, Kwon YH, Ts'o D, et al. Visual stimulus induced changes in human near-infrared fundus reflectance. *Invest Ophthalmol Vis Sci*. 2006;47:715–721.
3. Yao X-C, George JS. Dynamic neuroimaging of retinal light responses using fast intrinsic optical signals. *Neuroimage*. 2006;33:898–906.
4. Yao X-C, Zhao Y-B. Optical dissection of stimulus-evoked retinal activation. *Opt Express*. 2008;16:12446–12459.
5. Schallek J, Li H, Kardon R, et al. Stimulus-evoked intrinsic optical signals in the retina: spatial and temporal characteristics. *Invest Ophthalmol Vis Sci*. 2009;50:4865–4872.
6. Schallek J, Kardon R, Kwon Y, et al. Stimulus-evoked intrinsic optical signals in the retina: pharmacologic dissection reveals outer retinal origins. *Invest Ophthalmol Vis Sci*. 2009;50:4873–4880.
7. Schallek J, Ts'o D. Blood contrast agents enhance intrinsic signals in the retina: evidence for an underlying blood volume component. *Invest Ophthalmol Vis Sci*. 2011;52:1325–1335.
8. Ts'o D, Schallek J, Kwon Y, et al. Noninvasive functional imaging of the retina reveals outer retinal and hemodynamic intrinsic optical signal origins. *Jpn J Ophthalmol*. 2009;53:334–344.
9. Li Y-G, Zhang Q-X, Liu L, Amthor FR, Yao X-C. High spatiotemporal resolution imaging of fast intrinsic optical signals activated by retinal flicker stimulation. *Opt Express*. 2010;18:7210–7218.
10. Grieve K, Roorda A. Intrinsic signals from human cone photoreceptors. *Invest Ophthalmol Vis Sci*. 2008;49:713–719.
11. Hanazono G, Tsunoda K, Kazato Y, Tsubota K, Tanifuji M. Evaluating neural activity of retinal ganglion cells by flash-evoked intrinsic signal imaging in macaque retina. *Invest Ophthalmol Vis Sci*. 2008;49:4655–4663.
12. Del Sole MJ, Sande PH, Bernades JM, Aba MA, Rosenstein RE. Circadian rhythm of intraocular pressure in cats. *Vet Ophthalmol*. 2007;10:155–161.
13. Ohzawa I, Freeman RD. Pattern evoked potentials from the cat's retina. *J Neurophysiol*. 1985;54:691–700.
14. Bach M, Hawlina M, Holder GE, et al. Standard for pattern electroretinography: International Society for Clinical Electrophysiology of Vision. *Doc Ophthalmol*. 2000;101:11–18.
15. Lalezary M, Medeiros FA, Weinreb RN, et al. Baseline optical coherence tomography predicts the development of glaucomatous change in glaucoma suspects. *Am J Ophthalmol*. 2006;142:576–582.
16. Weber AJ, Harman CD, Viswanathan S. Effects of optic nerve injury, glaucoma, and neuroprotection on the survival, structure, and function of ganglion cells in the mammalian retina. *J Physiol*. 2008;586:4393–4400.

17. Weber AJ, Viswanáthan S, Ramanathan C, Harman CD. Combined application of BDNF to the eye and brain enhances ganglion cell survival and function in the cat after optic nerve injury. *Invest Ophthalmol Vis Sci*. 2010;51:327–334.
18. Miller PE, Pickett JP, Majors LJ, Kurzman ID. Evaluation of two applanation tonometers in cats. *Am J Vet Res*. 1991;52:1917–1921.
19. Rusanen E, Florin M, Hässig M, Spiess BM. Evaluation of a rebound tonometer (Tonovet) in clinically normal cat eyes. *Vet Ophthalmol*. 2010;13:31–36.
20. Vakkur GJ, Bishop PO, Kozak W. Visual optics in the cat, including posterior nodal distance and retinal landmarks. *Vis Res*. 1963;3:289–314.
21. Enroth-Cugell C, Shapley RM. Adaptation and dynamics of cat retinal ganglion cells. *J Physiol (Lond)*. 1973;233:271–309.
22. Enroth-Cugell C, Robson JG. Functional characteristics and diversity of cat retinal ganglion cells: basic characteristics and quantitative description. *Invest Ophthalmol Vis Sci*. 1984;25:250–267.
23. Blake R, Antoinetti DN. Abnormal visual resolution in the Siamese cat. *Science*. 1976;194:109–110.
24. Hubel DH, Wiesel TN. Aberrant visual projections in the Siamese cat. *J Physiol (Lond)*. 1971;218:33–62.
25. Stone J, Campion JE, Leicester J. The nasotemporal division of retina in the Siamese cat. *J Comp Neurol*. 1978;180:783–798.
26. Chino YM, Shansky MS, Hamasaki DI. Properties of X- and Y-type retinal ganglion cells in Siamese cats. *Brain Res*. 1978;143:459–473.
27. Chino YM, Shansky MS, Hamasaki DI. Siamese cats: abnormal responses of retinal ganglion cells. *Science*. 1977;197:173–174.
28. Stone J, Rowe MH, Campion JE. Retinal abnormalities in the Siamese cat. *J Comp Neurol*. 1978;180:773–782.
29. Stone J, Campion JE. Estimate of the number of myelinated axons in the cat's optic nerve. *J Comp Neurol*. 1978;180:799–806.
30. Thibos LN, Levick WR, Morstyn R. Ocular pigmentation in white and Siamese cats. *Invest Ophthalmol Vis Sci*. 1980;19:475–486.
31. Wen GY, Wisniewski HM, Sturman JA. Hereditary abnormality in tapetum lucidum of the Siamese cats. *Histochemistry*. 1982;75:1–9.